# High Yield of Long-Lived B-Side Charge Separation at Room Temperature in Mutant Bacterial Reaction Centers

**Arlene L. M. Haffa, Su Lin, JoAnn C. Williams, Aileen K. W. Taguchi, James P. Allen, and Neal W. Woodbury***

*Department of Chemistry and Biochemistry and Center for the Study of Early Events in Photosynthesis, Arizona State University, Tempe, Arizona 85287-1604*

*Received: March 18, 2003; In Final Form: June 26, 2003*

The photosynthetic reaction center of *Rhodobacter* (*Rb.*) *sphaeroides* is a quasi-symmetric pigment protein complex. This near symmetry results in two potential pathways for light-induced electron transfer, labeled A and B, yet under most conditions charge separation occurs almost exclusively along the A-side cofactors in wild-type reaction centers. One exception is that upon excitation with blue light (390 nm) a transient B-side charge-separated state, $B_B^+H_B^-$ (the cation of the B-side monomer bacteriochlorophyll and the anion of the B-side bacteriopheophytin), is formed that decays in picoseconds at room temperature but is stable at cryogenic temperatures. To characterize the nature of this reaction further, a series of mutations involving the introduction of potentially negative amino acids in the vicinity of P and the monomer bacteriochlorophylls, $B_A$ and $B_B$, were used to alter the local electrostatic environment. The most dramatic effects were observed for reaction centers with the mutations L168 His to Glu and L170 Asn to Asp. These mutant reaction centers display a stable (hundreds of picoseconds) formation of $B_B^+H_B^-$ not only using 390-nm excitation but also upon direct excitation of the lowest excited singlet states of the reaction center bacteriopheophytins and bacteriochlorophylls at 740 and 800 nm, respectively. Reaction centers mutated at three sites—L168 His to Glu, L170 Asn to Asp and M199 Asn to Asp—were also found to form a stable $B_B^+H_B^-$ state following excitation at 390 nm but with an apparently lower yield. In the other mutant reaction centers studied, long-lived $B_B^+H_B^-$ formation was not observed using any excitation wavelength, though 390-nm excitation resulted in $B_B^+H_B^-$ formation followed by the decay of this state on the picosecond time scale, as is observed in wild type. Combining these results with past work demonstrates that there is a rich variety of photochemistry possible in the reaction center. Both the pathway and products of light-induced charge separation depend on the interplay between local electrostatic interactions and the nature of the excited states available at early times.

The photosynthetic bacterium *Rhodobacter* (*Rb.*) *sphaeroides* is capable of efficient solar energy transduction via a series of electron- and proton-transfer events that take place in the reaction center, an integral membrane pigment−protein complex. Both the structure and mechanism of the reaction center have been studied extensively. (See, for example, refs 1−5.) The structure consists of three protein subunits (L, M, and H) and 10 cofactors.[6,7] Nine of the 10 reaction center cofactors are arranged in a nearly $C_2$ symmetric fashion. These include a bacteriochlorophyll dimer ($P_A$ and $P_B$, generally abbreviated P), two accessory bacteriochlorophylls ($B_A$ and $B_B$), two bacteriopheophytins ($H_A$ and $H_B$), two quinones ($Q_A$ and $Q_B$), and a non-heme iron (Fe). These cofactors form two structurally similar electron-transfer pathways in the reaction center; those with the subscript A form one path, and those with the subscript B form the other. However, the $C_2$ symmetry is not exact. The detailed amino acid environment around the cofactors differs between the two sides, as does the placement of the 10th cofactor, a carotenoid.

Upon excitation of P to form P*, initial electron transfer along the A-side cofactors occurs with a time constant of a few picoseconds, forming $P^+H_A^-$ presumably via $P^+B_A^-$. In about 200 ps, a subsequent electron transfer forms $P^+Q_A^-$, and then on longer time scales, $P^+Q_B^-$ is formed. Direct excitation of the lowest excited singlet states of P, B, or H in wild-type reaction centers results in essentially no B-side electron transfer from P to either $B_B$ or $H_B$.[8−13]

The direction of electron transfer from P* is apparently controlled by the relative energetics of the states $P^+B_A^-$ and $P^+B_B^-$. In wild-type reaction centers, the state $P^+B_B^-$ is apparently above P* in energy, and $P^+B_A^-$ is at or below P* in energy, ensuring an essentially unidirectional electron-transfer reaction from the lowest excited singlet state of P. By altering the relative energetics of $P^+B_A^-$ and $P^+B_B^-$ through mutagenesis, it is possible to generate substantial amounts of $P^+B_B^-$ after direct excitation of P.[14−16]

It is also possible to observe electron transfer involving B-side cofactors by generating higher excited states of the reaction center, even in wild type.[17] Excitation with 390-nm pulses results in transient population of the state $B_B^+H_B^-$ that decays within 15 ps at room temperature but is stable for at least hundreds of picoseconds at low temperature. The mechanism of $B_B^+H_B^-$ formation in wild-type reaction centers upon 390-nm excitation is not understood. $B_B^+H_B^-$ may be formed directly from higher excited states using 390-nm excitation. Alternatively, the formation of vibrationally excited states during electronic excited-state relaxation may be critical. The nature of the activated intermediate that mediates the decay of $B_B^+H_B^-$ and makes the process temperature-dependent is also not understood.

* To whom correspondence should be addressed. E-mail: NWoodbury@asu.edu.

10.1021/jp034703p CCC: $25.00 © 2003 American Chemical Society
Published on Web 10/21/2003

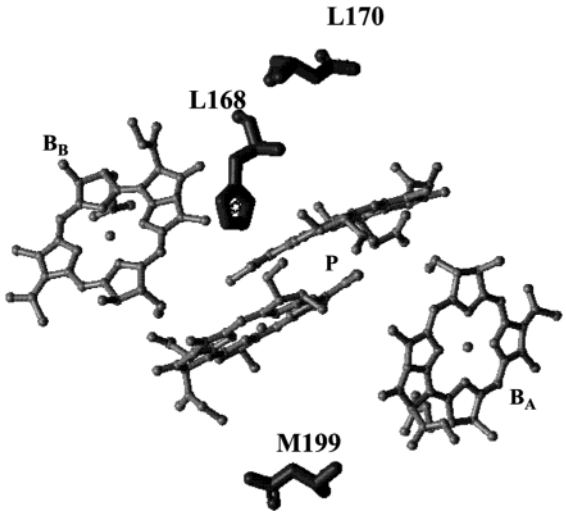


**Figure 1.** Structure of the reaction center from *Rhodobacter sphaeroides* showing the bacteriochlorophyll dimer (P), the two accessory bacteriochlorophylls ($B_A$ and $B_B$), and residues Asn M199, Asn L170, and His L168. The view is from the top down the approximate 2-fold symmetry axis of the protein.

In this report, the excitation wavelength dependence of electron transfer is considered in a recently described series of mutants[18] in which the electrostatic environment near P, $B_A$, and $B_B$ has been altered by placing potentially negatively charged amino acid residues nearby. This should perturb the energies of charge-separated states involving these cofactors, giving some insight into the role of thermodynamics in $B_B^+H_B^-$ formation and decay. Previously characterized mutations at three different residues have been used in this study. In the first, the His at L168 that forms a hydrogen bond to P in wild type[19] has been replaced with Glu (abbreviated L168HE, where the first letter indicates the protein subunit followed by the number of the amino acid residue and then the original and modified amino acids). The other two mutations involved placing aspartic acid residues at positions that should not directly affect the hydrogen bonding between P and the protein (L170ND and M199ND) but should affect the electrostatics in the region. The position of these amino acids relative to P is shown in Figure 1. It is not possible to measure directly the effects of these mutations on the midpoint potentials of the monomer bacteriochlorophylls, but measurements of the $P/P^+$ midpoint potentials in these mutants show a substantial decrease in each case compared to those of wild type.[18] These three single mutants and the four possible double and triple mutants have been constructed and characterized, including determining the $P/P^+$ midpoint potentials (Table 1 and ref 18), the ground-state absorption spectra, and the initial electron-transfer rate constants upon direct excitation of P.[20] All of the mutations result in an increase in the rate of electron transfer along the A side but no observable B-side transfer when P* is formed by direct excitation near 860 nm. Here, the pathway and kinetics of electron transfer in these mutants after exciting higher-energy electronic states of the reaction center will be explored. This should shed light on the interplay between the energetics of excited and charge-separated states in the reaction center.

## Materials and Methods

Reaction centers from previously described mutants with low $P/P^+$ midpoint potentials and from wild-type *Rb. sphaeroides* were isolated[18,20] and suspended in 15 mM Tris-HCl, 0.025% LDAO, 1 mM EDTA (TLE), pH 8.0. For this study, all possible single, double, and triple combinations of mutations L168HE, L170ND, and M199ND were used. The $P/P^+$ oxidation potential of wild-type reaction centers at pH 8.0 is 503 mV. The decrease in the midpoint potential of each mutant reaction center is given in Table 1 and has been previously reported.[18] All measurements were performed at room temperature.

**TABLE 1: Experimental Conditions for the Low $P/P^+$ Midpoint Potential Mutants**

| strain[a] | $P/P^+$ $\Delta E_m$ mV[b] | excitation wavelengths nm | time scales used[c] |
|---|---|---|---|
| L170ND | −44 | 390 | 1 |
| M199ND | −48 | 390 | 1 |
| L168HE | −75 | 390/800 | 1/3 |
| L170ND/M199ND | −83 | 390/800 | 2/3 |
| L168HE/M199ND | −110 | 390/740/800 | 2/1/1 short |
| L168HE/L170ND | −127 | 390/740/800 | 1,2/4/1,5 |
| L168HE/L170ND/M199ND | −147 | 390 | 2 |

[a] Numbering and nomenclature as described in text. [b] Change in $P/P^+$ midpoint potential relative to wild type ($P/P^+$ $\Delta E_m$) ± 5 mV, previously published.[18,20] [c] (1) −1 to 10 ps in 110 steps followed by 60 steps of 10 ps; (2) −1 to 10 ps in 110 steps followed by 50 steps of 20 ps; (3) −2 to 20 ps in 100 steps followed by 50 steps of 20 ps; (4) −200 to 2000 ps in 55 steps; (5) −10 to 20 ps in 15 steps followed by 10 steps of 100 ps.

**Transient Absorption Spectroscopy.** The apparatus used for subpicosecond-resolution transient absorption spectroscopy has been described previously.[17,21] After the addition of 1 mM 1,10-orthophenanthroline to block electron transfer from $Q_A$ to $Q_B$, the sample was placed in a spinning wheel with an optical path length of 2.5 mm. For each of the excitation wavelengths used (800, 740, or 390 nm) the pulse energy was between 1.5 and 2 $\mu$J. The diameter of the beam was 1 mm, and its spectral bandwidth (full width at half-maximum) was 5 nm with a temporal duration of ∼150 fs. Two sets of data were acquired for all of the mutant reaction centers using excitation at 390 nm and probing over spectral ranges from 480 to 780 nm and 730 to 1025 nm. Direct excitation of the bacteriochlorophyll monomers and the bacteriopheophytins was performed on selected samples (Table 1). Data following 800-nm excitation of L168HE, L170ND/M199ND, L168HE/M199ND, and L168HE/L170ND and 740-nm excitation of L168HE/M199ND and L168HE/L170ND reaction centers were also acquired. All measurements were taken on two time scales to resolve both the initial and long-time photochemistry (Table 1). Spectral dispersion at early times was empirically corrected,[22] and data analysis of the transient absorbance surfaces (time vs wavelength) was performed as previously described[23] using locally written software (ASUFIT) developed under a MATLAB environment (Mathworks Inc., the locally written analysis software is available electronically upon request[14]).

## Results

Transient absorption changes in both the $Q_x$ and the $Q_y$ regions were measured using 800-, 740-, and 390-nm excitation pulses in a series of mutants. The mutants have amino acid residues that are potentially negatively charged in the vicinity of P and the monomer bacteriochlorophylls. This clearly changes the electrostatic environment in the region as the $P/P^+$ midpoint potentials are decreased by 44 to 147 mV below that of wild type (Table 1 and ref 18). The midpoint potentials of the monomer bacteriochlorophylls are presumably changed as well, but it is not possible to measure these directly.

**Distinguishing between A- and B-Side Electron Transfer.** Discrimination between A- and B-side electron transfer in the

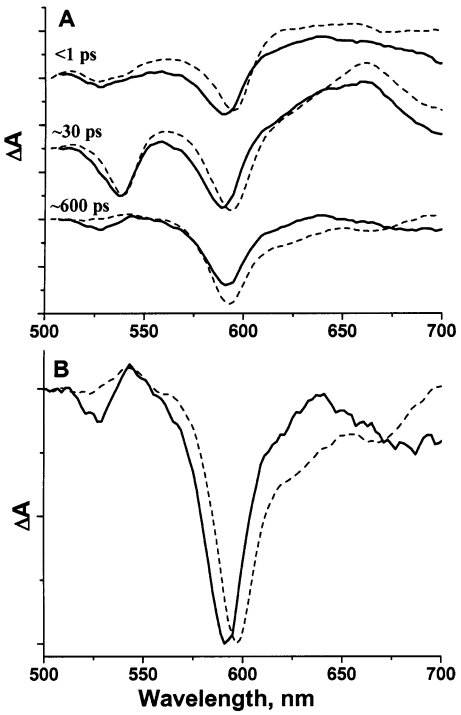


**Figure 2.** (A) Time-resolved spectra of wild type (--) and L168HE/L170ND (—) reaction centers following excitation at 740 nm. The top traces are at <1 ps after excitation, the middle traces are at ~30 ps, and the bottom traces are at ~600 ps. The traces have been reconstructed from a fit, corrected for dispersion effects as described in Materials and Methods, and normalized to the magnitude of the bleaching of the $Q_x$ transition near 540 nm at intermediate times (~30 ps). The two traces at each time point have been shifted vertically such that they are equal at 510 nm. Traces at different time points are offset for clarity. (B) Nondecaying component of the decay-associated spectra obtained from fits of data acquired for wild type (--) and L168HE/L170ND (—) reaction centers following excitation at 740 nm at room temperature. Traces have been normalized to the bleaching of the P/B $Q_x$ transition near 600 nm.

transient absorbance measurements performed here relies on the fact that the $Q_x$ absorption bands for the two bacteriopheophytins ($H_A$ and $H_B$) have slightly different transition energies. At low temperature, the two transitions are clearly resolved, with the $H_B$ transition centered at 535 nm and the $H_A$ transition centered at 545 nm.[24] At room temperature, these peaks are broader but do not completely overlap such that $H_B$ is centered near 530 nm and $H_A$ is near 540 nm. Upon the formation of $H_B^-$, there is an absorbance increase near 630 nm due to the anion.[25−27] The $Q_x$ absorption bands of P, $B_A$, and $B_B$ are superimposed near 600 nm, but the $Q_y$ transitions of P and the two monomer bacteriochlorophylls are distinguishable at 865 and 800 nm, respectively. In the mutants used here, with the exception of M199ND, the $Q_y$ P band shifts to the blue, in some cases by as much as 14 nm.[20] No shifts in the ground-state spectra for any of the other transitions were found at room or cryogenic temperatures.

**Direct Excitation of Monomer Bacteriochlorophyll and Bacteriopheophytin $Q_y$ Transitions.** Time-resolved spectra in the $Q_x$ region for wild-type and L168HE/L170ND reaction centers following excitation at 740 nm are shown in Figure 2A. Excitation at this wavelength favors the lowest excited state of $H_B$, although $H_A$ is also excited. The top traces in Figure 2A are at <1 ps, the middle traces are at ~30 ps, and the bottom traces are at ~600 ps.

To remove the effects of dispersion at early times, the data were fit to a sum of exponentials (see below), and this fit was then used as described previously[22,23] in conjunction with an empirical measurement of the dispersion to reconstruct an accurate description of the early-time kinetics. In this Figure (as well as in Figures 4 and 6), the data have been normalized to the magnitude of the bleaching of the $H_A$ $Q_x$ transition near 540 nm at intermediate times (~30 ps). This normalization between the samples is somewhat arbitrary because different final states are being formed in the different samples, thus there is no unique transition in common between them (described in detail later). The band near 540 nm at intermediate times was chosen because all samples appear to be forming at least some $P^+H_A^-$.

*Excitation at 740 or 800 nm in Wild Type.* In wild type, both $H_B$ (~530 nm) and $H_A$ (~540 nm) bleaching occurs within the duration of the excitation pulse (~150 fs) (Figure 2A, top trace) following 740-nm excitation. The ~540-nm band continues to grow in over several picoseconds (Figure 2A, middle trace), which is consistent with energy transfer from B and H to P on subpicosecond time scales followed by the formation of $P^+H_A^-$ on the picosecond time scale, as suggested previously.[28] The ~540-nm band then recovers over hundreds of picoseconds as the electron is transferred to $Q_A$ and the state $P^+Q_A^-$ is formed. (The resulting $P^+Q_A^-$ difference absorbance spectrum of wild type at 600 ps is shown in Figure 2A, bottom trace.) Excitation at 800 nm also results in $P^+Q_A^-$ on the same time scale (data not shown).

*Excitation at 740 or 800 nm in L168HE/L170ND Reaction Centers.* Both 800- and 740-nm excitation results in the formation of a long-lived state involving B-side cofactors in L168HE/L170ND reaction centers. Bleaching near 530 nm is evident at early times because of the direct excitation of $H_B$ at 740 nm, much as is seen in wild type (Figure 2A, top trace), and this is followed by the formation of $P^+H_A^-$ at intermediate times (Figure 2A, middle trace). However, in the L168HE/L170ND reaction centers, substantial bleaching of the $H_B$ ground state is still observed after 600 ps (Figure 2A, bottom trace). These spectral differences between the mutant and the wild type at long times are even more apparent when the data are globally fit to three exponential decay terms and a constant term and the difference spectrum of the final state is compared (Figure 2B). Only the nondecaying component of the fit differed substantially between wild type and the mutant; the three exponential decay terms were very similar both with regard to decay times and decay-associated spectra and included components with lifetimes of several hundred femtoseconds, a few picoseconds, and approximately 200 ps.[29] In L168HE/L170ND reaction centers, the nondecaying component shows a bleaching at 530 nm associated with the reduction of $H_B$ as well as an absorbance increase, particularly relative to wild type, near 630 nm. These spectral features have been observed previously and have been interpreted as $H_B^-$ formation (bleaching of the ground-state band of $H_B$ and formation of an anion band associated with $H_B^-$).[17] Using 800-nm excitation, very similar results are obtained (data not shown).

In the $Q_y$ region, 740-nm excitation rapidly results in 800-nm bleaching of the monomer bacteriochlorophyll band in concert with the bleaching of $H_B$ in the $Q_x$ region described above. Like the $H_B$ bleaching near 530 nm, the 800-nm absorbance decrease also remains on the 600-ps time scale (data not shown). The correlation between the ~530- and 800-nm bleaching will be described in more detail below for data obtained using 390-nm excitation. While there is clearly significant involvement of $H_B$ in the photochemistry upon 740- or 800-nm excitation in the L168HE/L170ND reaction centers,

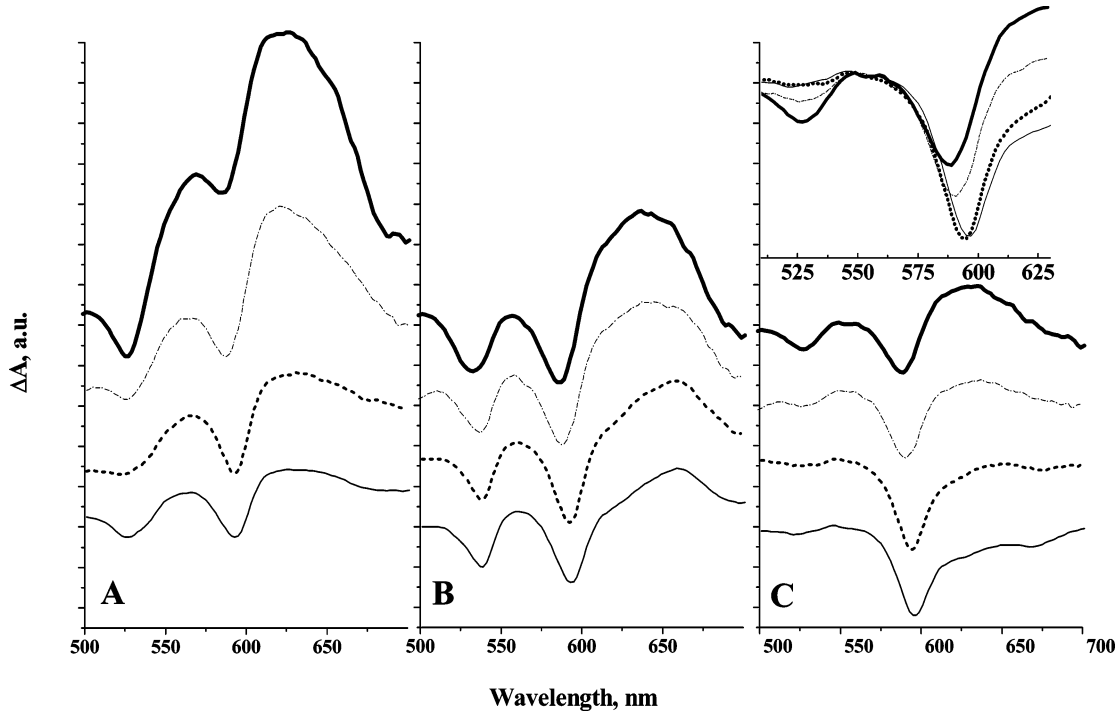


**Figure 3.** Transient absorbance spectra of wild-type and mutant reaction centers following 390-nm excitation at room temperature. (−) Wild type, (---) L170ND/M199ND, (- · -) L168HE/L170ND/M199ND, and (—) L168HE/L170ND. Data have been fit and normalized as in Figure 2. (A) Early-time-resolved spectra (≤1 ps) at the time of the largest signal near 630 nm. (B and C) Time-resolved spectra at ∼30 ps and ∼600 ps, respectively. (Inset) Expanded view of the $Q_x$ spectral region near the $H_A$ and $H_B$ transitions at ∼600 ps. Traces in the inset are not offset as they are in A−C.

most of the photochemistry in this mutant still results in long-lived A-side charge separation. As a result of this A-side photochemistry, the bleaching near 590 nm, which is due to the mixture of $B_B^+$ and $P^+$, is larger at 600 ps than the bleaching near 530 nm due to $H_B^-$.

*Excitation at 800 or 740 nm in Most Other Mutants Does Not Result in Long-Lived B-Side Charge Separation.* Transient absorbance measurements using 800- or 740-nm excitation were performed on a number of the other mutant reaction centers as well (Table 1). Following the excitation of L168HE, L168HE/M199ND, or L170ND/M199ND reaction centers at 800 nm or L170ND/M199ND or L168HE/M199ND reaction centers at 740 nm, only A-side charge separation forming $P^+H_A^-$ and $P^+Q_A^-$ is observed at intermediate and long times, respectively (data not shown).

**Blue Light Excitation.** Blue light excitation (390 nm) was studied in the entire series of mutants. Figure 3 shows examples of time-resolved spectra (wild type, L168HE/L170ND, L170ND/M199ND, and L168HE/L170ND/M199ND). Panel A (≤ 1 ps) shows spectra at the time of the largest absorbance increase near 630 nm, panel B (∼30 ps) shows spectra at the time that the formation of $P^+H_A^-$ is complete, and panel C (∼600 ps) shows data after the electron on $P^+H_A^-$ has progressed to form $P^+Q_A^-$ on the A side. Data are offset to show details except for the inset of panel C, which is overlaid so that differences in the magnitude of the signals at long times may be more easily observed.

*Early-Time Absorbance Changes upon 390-nm Excitation.* Figure 3A shows dispersion-corrected, subpicosecond transient difference spectra at room temperature that are normalized to the bleaching of the ∼540-nm ground-state transition of $H_A$ at ∼30 ps. In the difference spectra for all of the reaction centers, at least some bleaching near 530 nm ($H_B$) and some absorbance increase near 630 nm are observed within a few hundred femtoseconds of excitation at 390 nm, though the amount is quite variable (Figure 3A). Of the reaction center samples shown in Figure 3A, L168HE/L170ND reaction centers show the largest absorbance changes, L168HE/L170ND/M199ND reaction centers give intermediate results, and L170ND/M199ND reaction centers show absorbance changes similar in magnitude to those of wild type. There is also bleaching at 585−595 nm (depending on the mutant), which is apparently due at least in part to $B_B^+$ formation, as determined by looking at absorbance changes in the $Q_y$ region of the spectrum. (See below and ref 17.) In addition to variability in the overall size of the absorbance changes in this region, the relative size of the ∼530-nm bleaching and the anion band at ∼630 nm appears to vary from mutant to mutant. (Compare, for example, L168HE/L170ND/M199ND reaction centers and wild type in Figure 3A.) However, there is spectral overlap in this region with absorbance changes from excited states, and the recovery of these absorbance changes is extremely rapid in some of the mutants, making the initial amplitudes difficult to measure accurately.

*Time Evolution of Absorbance Changes upon 390-nm Excitation.* In wild type and all of the mutant reaction centers except L168HE/L170ND/M199ND and L168HE/L170ND, the bleaching near 530 nm and absorbance increase at ∼630 nm evolve within ∼15 ps to have the shape of the spectrum associated with $P^+H_A^-$, including bleaching at ∼540 nm ($H_A$), an absorbance increase centered near 660 nm ($H_A^-$), and bleaching near 595 nm ($P^+$) (Figure 3B and ref 17). The transient spectra from reaction center mutants L168HE/L170ND/M199ND and L168HE/L170ND, however, have, in addition to the $P^+H_A^-$ spectral features described above, residual ground-state bleaching near 530 nm and a substantial absorbance increase near 630 nm, indicative of $H_B^-$. In wild type and all of the mutant reaction centers, further electron transfer then occurs over hundreds of picoseconds, forming $P^+Q_A^-$ (Figure 3C). At this time, in both

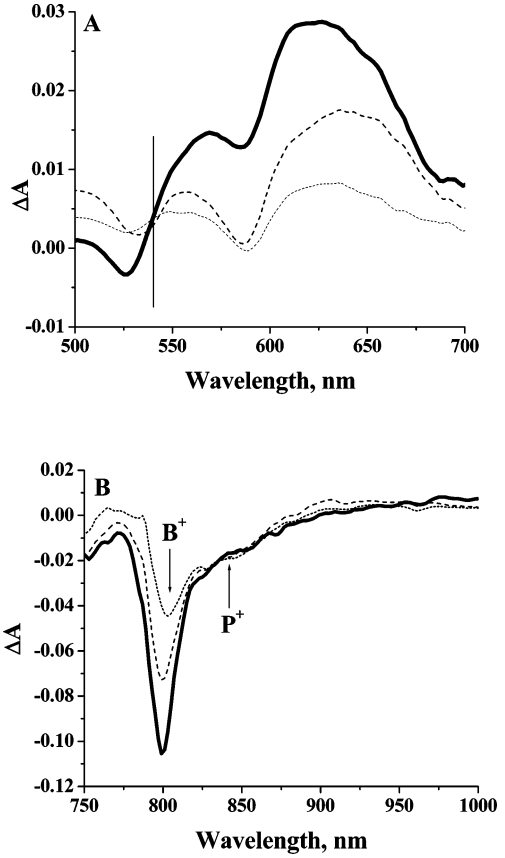


**Figure 4.** Time-resolved spectra in the (A) $Q_x$ region and the (B) $Q_y$ region for L168HE/L170ND reaction centers following excitation at 390 nm. Data have been reconstructed from a fit and corrected for dispersion as described in Materials and Methods. (—) <1 ps, (--) ~30 ps, and (···) ~600 ps. In A, a vertical line is shown at 540 nm, the center of the $H_A$ ground-state transition.

wild type and L170ND/M199ND reaction centers, there is almost no remaining bleaching of either $H_A$ or $H_B$ (~540 or ~530 nm). In fact, the only prominent feature that remains in the entire $Q_x$ region is the bleaching near 595 nm due to the formation of $P^+$, as would be expected for the state $P^+Q_A^-$. In contrast, although roughly half of the early-time absorbance changes associated with $H_B^-$ decays in tens of picoseconds, the other half still persists at 600 ps in L168HE/L170ND and L168HE/L170ND/M199ND reaction centers. Both samples still show ~530-nm bleaching and a ~630-nm absorbance increase associated with $H_B^-$ (Figure 3C). The size of these absorbance changes, relative to the absorbance change at 585 nm, is clearly smaller in L168HE/L170ND/M199ND reaction centers than in L168HE/L170ND reaction centers (roughly 50%).

*A- and B-Side Charge-Separated States in L168HE/L170ND Reaction Centers upon 390-nm Excitation.* Reaction centers isolated from the mutant L168HE/L170ND display some A-side photochemistry when excited at 390 nm, as can be seen most clearly in the bacteriopheophytin $Q_x$ region of the spectrum where $H_B$ and $H_A$ absorb (Figure 4A). A vertical line has been placed on the abscissa where the $H_A$ transition should occur (540 nm). There are shifts in the position of the bleaching of the bacteriopheophytin band from ~527 nm at early times to 530 nm on intermediate time scales, suggesting that there is some growing in of the red side ($H_A$ side) of the bleaching, as would be expected during the formation of $P^+H_A^-$. The center of the bacteriopheophytin ground-state bleaching returns to ~527 nm at longer times, indicative of the further electron transfer from $H_A$ to $Q_A$, leaving only the $H_B$ bleaching due to $B_B^+H_B^-$ by 600 ps.

In the $Q_y$ region of the spectrum (Figure 4B), the ground-state transitions of the monomer bacteriochlorophylls and P are well separated at 800 and 849 nm, respectively, in L168HE/L170ND reaction centers. (The P bleaching is substantially blue-shifted from the wild-type value of 865 nm.[20]) Excitation at 390 nm results in a long-lived bleaching at 800 nm that dominates the absorbance changes in this spectral region at all times measured. The P bleaching near 849 nm though present is smaller and does not change over the time scales measured. With time, 800-nm bleaching decreases, consistent with the decrease observed in ~530-nm ground-state bleaching and the ~630-nm absorbance increase associated with $H_B^-$.

## Discussion

Transient difference absorption spectroscopy was used to monitor electron-transfer events following excitation at 800, 740, and 390 nm in a series of reaction-center mutants in which the electrostatic environment of the cofactors involved in initial charge separation has been perturbed. Excitation at 800 nm should generate the lowest excited singlet states of both monomer bacteriochlorophylls. Excitation at 740 nm should generate the lowest excited singlet states of the two bacteriopheophytins, with a preference for $H_B$. Excitation at 390 nm potentially generates higher excited states of all of the bacteriochlorophylls and bacteriopheophytins in the reaction center, though past work suggests that P is not excited at this wavelength.[17] Excitation at 390 nm in wild type has been shown to generate the charge-separated state $B_B^+H_B^-$.[17] In wild type, this state decays in <15 ps at room temperature, whereas at 10 K it is stable for hundreds of picoseconds.

The series of mutations used in this study includes the symmetry-related mutations L170ND and M199ND, which place potentially negatively charged amino acid residues near the cofactors involved in initial electron transfer and thus may change the electrostatic fields in that region. Also, the mutation L168HE was used, which may have similar electrostatic effects and/or may remove a hydrogen bond from the dimer.[19,30] Previous work has shown that each of these mutations results in pH-dependent stabilization of $P^+$, lowering the $P/P^+$ midpoint potential at pH 8.0 by as much as 147 mV when all three mutations are present (Table 1).[31] This is consistent with the concept that these mutations introduce negative charges in the vicinity of the cofactors involved in initial electron transfer.

**Electron-Transfer Pathway Depends on Excitation Wavelength.** In wild type, essentially all charge separation for which P serves as the initial electron donor utilizes the A-side cofactors. Previous measurements on the current series of mutants also resulted in the observation of only A-side charge separation upon the excitation of P.[20] This unidirectional charge separation is apparently due to the relative free energy of the states $P^+B_A^-$ and $P^+B_B^-$. A number of mutants have been made previously in which the free energy of $P^+B_B^-$ has been decreased or that of $P^+B_A^-$ increased or both, allowing substantial amounts of electron transfer from P to $B_B$ or $H_B$ to occur.[14−16] (In some of these cases, $B_B$ has been substituted with bacteriopheophytin to make it easier to reduce.)

Excitation at 740 and 800 nm resulted in predominantly A-side photochemistry in all of the mutants studied here, generating $P^+H_A^-$ on the picosecond time scale followed by the formation of $P^+Q_A^-$ in hundreds of picoseconds (e.g., Figure 3), as is observed in wild type.[13,29,32,33] In those mutant reaction

centers tested other than L168HE/L170ND, neither 800- nor 740-nm excitation resulted in any long-lived B-side charge-separated states. At early times, there were subtle spectral characteristics such as the transient rise near 630 nm in Figure 3, suggestive of the involvement of the B-side cofactors, but no clear assignment of B-side charge separation can be made using these excitation energies. In any case, none of these signals persisted longer than 1 ps.

In contrast, 740- and 800-nm excitation of L168HE/L170ND reaction centers resulted in detectable long-lived $B_B^+H_B^-$ formation (at least hundreds of picoseconds). The spectral changes associated with $B_B^+H_B^-$ include a rise in the 630-nm region (due in part to an $H_B$ anion) and bleaching near 530 nm ($H_B$ ground state) and 800 nm (due in part to $B_B$). The differences in the absorbance changes in these spectral regions between reaction centers from wild type and L168HE/L170ND are small compared to the total signal at early and intermediate times (Figure 2A top and middle traces). It is only on longer time scales (Figure 2A bottom traces and 2B) that the differences between these two types of reaction centers become apparent, and clear evidence for the long-lived formation of B-side charge separation can be seen. This is because the absorbance changes associated with B-side electron transfer involve bleaching near 530 nm and an absorbance increase near 630 nm due to $H_B^-$ formation, and these signals overlap with the absorbance changes due to $H_A^-$ formation. After the $H_A^-$ signals have decayed because of electron transfer from $H_A$ to $Q_A$, the $H_B^-$ absorbance changes become clear under these excitation conditions (Figure 2A bottom traces and 2B).

Blue light (390 nm) excitation of all of the mutants studied here, as seen previously for wild type,[17] results in absorbance changes at early times involving B-side cofactors (Figures 3A and 4A) including bleaching near 530 nm (the $H_B$ ground-state $Q_x$ transition), 600 nm (bacteriochlorophyll $Q_x$ transition), and 800 nm (monomer bacteriochlorophyll $Q_y$ transition, Figure 4B) with an additional absorbance increase near 630 nm (presumably due to an anion absorbance of $H_B^-$, Figures 3A and 4A). Although the bleaching near 530 nm is less pronounced in some of the mutants, all of the mutants display $H_B$ anion characteristics. Taken together, these absorbance changes suggest that within the first picosecond at least some $B_B^+H_B^-$ is formed upon 390-nm excitation in addition to the A-side charge separation mentioned above in all of the mutants. This is similar to previous conclusions for wild-type reaction centers.[17]

**Yield of B-Side Charge Separation.** The two reaction-center mutants with the most prominent absorbance changes involving B-side cofactors upon 390-nm excitation are L168HE/L170ND and L168HE/L170ND/M199ND. If one normalizes the data based on the size of the $Q_x$ $H_A$ transition bleaching near 540 nm when it is the greatest (~30 ps, Figure 3B) and then compares the relative amount of bleaching near 530 nm at long times (Figure 3C), there is apparently more than twice as much B-side charge separation in L168HE/L170ND reaction centers relative to those from L168HE/L170ND/M199ND reaction centers. This yield estimate is only approximate because the normalization relies on separating two overlapping transitions and this method assumes that $P^+H_A^-$ and $B_B^+H_B^-$ are the only possible products of excitation at this wavelength. However, there is clearly substantially more of the B-side charge-separated state formed in the L168HE/L170ND reaction centers than in L168HE/L170ND/M199ND reaction centers and more in either of these mutant reaction centers than in any of the others.

One can also estimate the A- to B-side branching ratio upon 390-nm excitation for L168HE/L170ND reaction centers by comparing the absorbance changes measured when exciting at this wavelength with those observed from previous measurements taken using 850-nm excitation. Transient spectra at ~30 ps using 390- and 850-nm excitation are compared in Figure 5. Excitation at 850 nm results in only the bleaching of the $H_A$ ground-state transition at 540 nm (Figure 5 and ref 20). In contrast, the bleaching of the $H_A$ (540 nm) and $H_B$ (~530 nm) $Q_x$ ground-state absorption bands at ~30 ps appears to be approximately equal using 390-nm excitation, suggesting a branching ratio between the two sides of roughly 50:50. This may be an underestimate of the B-side yield, however, because by 30 ps some of the B-side anion has recovered and presumably all of the A-side charge-separated products have formed.

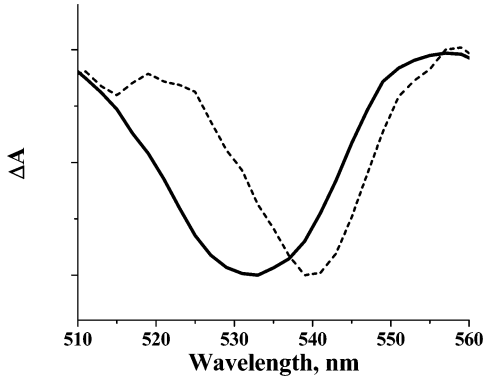


**Figure 5.** Comparison of transient absorbance spectra recorded approximately 30 ps after 850-nm (--) and 390-nm (−) excitation in L168HE/L170ND reaction centers at room temperature. Data have been reconstructed from a fit, dispersion corrected as described in Materials and Methods, and normalized as described in Figure 2. Data using 850-nm excitation are taken from ref 20.

**Decay Kinetics of $B_B^+H_B^-$ is Altered in Mutants with Ionizable Residues Near the Primary Electron Donor.** The introduction of potentially negatively charged amino acids in the vicinity of the cofactors involved in initial electron transfer clearly affects the decay kinetics of the $B_B^+H_B^-$ state once it is formed. In wild type and in most of the mutants studied, the decay of $B_B^+H_B^-$ is rapid, being complete within 15 ps at room temperature. In fact, in at least some of these mutants (those containing M199ND, see Table 1), the recovery of the B-side charge-separated state appears to be slightly faster than that of wild type, though the complexity of the very early time dynamics makes it difficult to determine the kinetics of this process accurately. In stark contrast, the decay of $B_B^+H_B^-$ in the L168HE/L170ND and L168HE/L170ND/M199ND reaction-center mutants occurs much more slowly and on multiple time scales with a substantial amount of the state still being present after 600 ps (Figures 2−4).

Apparently, $B_B^+H_B^-$, once formed, is stable at room temperature in a subpopulation of L168HE/L170ND and L168HE/L170ND/M199ND reaction centers. Although the amount remaining at long times is less in L168HE/L170ND/M199ND reaction centers than in L168HE/L170ND reaction centers, the longer decay time of the $B_B^+H_B^-$ that is formed appears to be quite similar. Thus, either the introduction of the local negative charges in these two mutants stabilizes $B_B^+H_B^-$ enough to slow its decay greatly at room temperature or they destabilize the activated intermediate through which this charge-separated state decays or both. The presence of such an activated intermediate has been shown previously in wild type by the fact that $B_B^+H_B^-$ is stable for at least hundreds of picoseconds at 10 K.[17]

In wild-type reaction centers, it was suggested that at least one active decay path of $B_B^+H_B^-$ involved the formation of

$P^+H_A^-$, possibly via recombination reforming an excited state.[17] However, in L168HE/L170ND reaction centers, recovery of the bleaching at 800 nm (presumably the decay of $B_B^+$) is not correlated with an increase in the bleaching of the P transition near 850 nm (resulting from the formation of $P^+H_A^-$, Figure 4B). At least in this mutant, $B_B^+H_B^-$ decay does not lead to $P^+H_A^-$ formation. In the other mutants studied, the situation is less clear, but the anion band signal at ~660 nm due to $H_A^-$ apparently does not increase with the same kinetics with which the $H_B^-$ anion signal at ~630 nm decays, again suggesting that the decay of $B_B^+H_B^-$ does not give rise to additional $P^+H_A^-$ formation in these mutants.

**Role of Static Charge Distribution in Determining $B_B^+H_B^-$ Stability.** For B-side charge separation, the pathway and stability depend on the excitation wavelength and the amino acid environment. The lowering of the midpoint potential of P[18] and most likely B because of the introduction of potentially negatively charged amino acid residues is not likely the sole determining factor in the stability of $B_B^+H_B^-$ . If the midpoint potentials were the sole determining factor, then one would expect that L168HE/L170ND/M199ND reaction centers should have a greater amount of B-side charge separation than L168HE/L170ND at long times, contrary to observation (Figure 3). In principle, the L168HE/L170ND/M199ND mutant introduces three negative charges in the region instead of two for the L168HE/L170ND mutant. In fact, the addition of M199ND to L168HE and L170ND seems to *decrease* the amount of $B_B^+H_B^-$ that is stable at hundreds of picoseconds. It may be that the distribution of charges is as important as the electrostatic effects on the thermodynamics of charge separation. Because M199ND and L170ND are symmetric mutations, depending on whether one, the other, or both are charged, the polarity and magnitude of the electric field gradient in the vicinity should change. This could affect, for example, the transition dipole moment of P or the P/P* difference dipole, which in turn may alter the competition between energy transfer from $B_B$* or $H_B$* to P versus direct charge separation from $B_B$* or $H_B$* forming $B_B^+H_B^-$.

The pH dependences of the $P/P^+$ midpoint potentials of M199ND,[18] L168HE, L170ND, and L168HE/L170ND (unpublished results) reaction centers result in an approximate p$K_A$ of 8 for each mutant. Thus, at pH 8, one might expect that on the femtosecond to picosecond time scale the reaction centers will be heterogeneous with respect to the protonation state of the different amino acid residues involved. This likely gives rise to some of the complexity observed in the transient absorbance changes. Studies of the pH dependence of the pathway and kinetics of electron transfer in this series of mutants will be published elsewhere.

**Electron-Transfer Pathways in Reaction Centers.** Both this work and a number of previous studies[17,34−37] have shown that there is a rich variety of photochemistry that can occur in the bacterial photosynthetic reaction center. Under the excitation conditions used in this report, both A- and B-side charge-separated states ($P^+H_A^-$ or $P^+Q_A^-$, and $B_B^+H_B^-$) can be formed in wild-type reaction centers, but at room temperature, only the A-side charge-separated states are stable.[17] Furthermore, in wild type, excitation at 390 nm is necessary to observe $B_B^+H_B^-$, and this state is only transiently present at room temperature. In the mutant L168HE/L170ND, where potentially negatively charged amino acid residues have been introduced in the vicinity of the initial electron-transfer reactions, the energetics has apparently been changed enough so that lower-energy excitation (740 and 800 nm compared to 390 nm) can give rise to long-lived $B_B^+H_B^-$ (at least hundreds of picoseconds). The ability to generate long-lived $B_B^+H_B^-$ at room temperature in L168HE/L170ND reaction centers should provide a useful system for detailed studies of this charge-separated state.

**Acknowledgment.** This work was supported by the National Science Foundation (grants MCB-9817388, MCB-0131776, and BIR9512970) and the U. S. Department of Agriculture (grant 1999-01753). ALMH was supported by a graduate research training grant from the National Science Foundation (DGE-9553456). This is publication no. 576 from the Center for the Study of Early Events in Photosynthesis.

## References and Notes

(1) Gunner, M. *Curr. Top. Bioenerg.* **1991**, *16*, 319−367.
(2) Kirmaier, C.; Holten, D. Electron Transfer and Charge Recombination Reactions in Wild-Type and Mutant Bacterial Reaction Centers. In *The Photosynthetic Reaction Center*; Deisenhofer, J., Norris, J. R., Eds.; Academic Press: San Diego, CA, 1993; Vol. 2, pp 49−70.
(3) Parson, W. W. Photosynthetic Bacterial Reaction Centres. In *Protein Electron Transfer*; Bendall, S. D., Ed.; BIOS Scientific Publishers: Oxford, England, 1996; pp 125−160.
(4) Hoff, A. J.; Deisenhofer, J. *Phys. Rep.* **1997**, *287*, 2−247.
(5) Cogdell, R.; Lindsay, J. G. *New Phytologist* **2000**, *145*, 167−196.
(6) Allen, J. P.; Feher, G.; Yeates, T. O.; Komiya, H.; Rees, D. C. *Proc. Natl. Acad. Sci. U.S.A.* **1987**, *84*, 5730−5734.
(7) Allen, J. P.; Feher, G.; Yeates, T. O.; Komiya, H.; Rees, D. C. *Proc. Natl. Acad. Sci. U.S.A.* **1988**, *85*, 8487−8491.
(8) Kirmaier, C.; Holten, D.; Parson, W. W. *Biochim. Biophys. Acta* **1985**, *810*, 49−61.
(9) Kirmaier, C.; Holten, D.; Parson, W. W. *Biochim. Biophys. Acta* **1985**, *810*, 33−48.
(10) Breton, J.; Martin, J.-L.; Migus, A.; Antonetti, A.; Orszag, A. Femtosecond Spectroscopy of Excitation Energy Transfer and Initial Charge Separation in the Reaction Center of the Photosynthetic Bacterium *Rhodopseudomonas sphaeroides*. In *Ultrafast Phenomena V*; Fleming, G. R., Siegman, A. E., Eds.; Springer-Verlag: New York, 1986.
(11) Walker, G. C.; Maiti, S.; Reid, G. D.; Wynne, K.; Moser, C. C.; Pippenger, R. S.; Cowen, B. R.; Dutton, P. L.; Hochstrasser, R. M. Femtosecond Infrared Spectroscopy of the Photosynthetic Reaction Center. In *Ultrafast Phenomena IX*; Barbara, P. F., Ed.; Springer: Berlin, 1994.
(12) Jia, Y.; Jonas, D. M.; Joo, T.; Nagasawa, Y.; Lang, M. J.; Fleming, G. R. *J. Phys. Chem.* **1995**, *99*, 6263−6266.
(13) Stanley, R. J.; King, B.; Boxer, S. G. *J. Phys. Chem.* **1996**, *100*, 12052−12059.
(14) Katilius, E.; Turanchik, T.; Lin, S.; Taguchi, A. K. W.; Woodbury, N. W. *J. Phys. Chem. B* **1999**, *103*, 7386−7389.
(15) Kirmaier, C.; He, C.; Holten, D. *Biochemistry* **2001**, *40*, 12132−12139.
(16) Katilius, E.; Katiliene, Z.; Lin, S.; Taguchi, A. K. W.; Woodbury, N. W. *J. Phys. Chem. B* **2002**, *106*, 1471−1475.
(17) Lin, S.; Katilius, E.; Haffa, A. L. M.; Taguchi, A. K. W.; Woodbury, N. W. *Biochemistry* **2001**, *40*, 13767−13773.
(18) Williams, J. C.; Haffa, A. L. M.; McCulley, J. L.; Woodbury, N. W.; Allen, J. P. *Biochemistry* **2001**, *40*, 15403−15407.
(19) Lancaster, C. R. D.; Bibikova, M. V.; Sabatino, P.; Oesterhelt, D.; Michel, H. *J. Biol. Chem.* **2000**, *275*, 39364−39368.
(20) Haffa, A. L. M.; Lin, S.; Katilius, E.; Williams, J. C.; Taguchi, A. K. W.; Allen, J. P.; Woodbury, N. W. *J. Phys. Chem. B* **2002**, *106*, 7376−7384.
(21) Freiberg, A.; Timpmann, K.; Ruus, R.; Woodbury, N. W. *J. Phys. Chem. B* **1999**, *103*, 10032−10041.
(22) Greene, B. I.; Farrow, R. C. *Chem. Phys. Lett.* **1983**, *98*, 273−276.
(23) Tang, C.-K.; Williams, J. C.; Taguchi, A. K. W.; Allen, J. P.; Woodbury, N. W. *Biochemistry* **1999**, *38*, 8794−8799.
(24) Kirmaier, C.; Holten, D. *Photosynth. Res.* **1987**, *13*, 225−260.
(25) Robert, B.; Lutz, M.; Tiede, D. M. *FEBS Lett.* **1985**, *183*, 326−330.
(26) Gray, K. A.; Wachtveitl, J.; Oesterhelt, D. *Eur. J. Biochem.* **1992**, *207*, 723−731.
(27) Heller, B. A.; Holten, D.; Kirmaier, C. *Science* **1995**, *269*, 940−945.
(28) Lin, S.; Jackson, J.; Taguchi, A. K. W.; Woodbury, N. W. *J. Phys. Chem. B* **1998**, *102*, 4016−4022.
(29) Lin, S.; Taguchi, A. K. W.; Woodbury, N. W. *J. Phys. Chem.* **1996**, *100*, 17067−17078.

(30) Spiedel, D.; Roszak, A. W.; McKendrick, K.; McAuley, K. E.; Fyfe, P. K.; Nabedryk, E.; Breton, J.; Robert, B.; Cogdell, R.; Isaacs, N. W.; Jones, M. R. *Biochim. Biophys. Acta* **2002**, *1554*, 75−9375−9392.

(31) Gunner, M.; Nicholls, A.; Honig, B. *J. Phys. Chem.* **1996**, *100*, 4277−4291.

(32) Breton, J.; Martin, J.-L.; Migus, A.; Antonetti, A.; Orszag, A. *Proc. Natl. Acad. Sci. U.S.A.* **1986**, *83*, 5121−5125.

(33) Jonas, D. M.; Lang, M. J.; Nagasawa, Y.; Joo, T.; Fleming, G. R. *J. Phys. Chem.* **1996**, *100*, 12660−12673.

(34) van Brederode, M. E.; Jones, M. R.; van Mourik, F.; van Stokkum, I. H. M.; van Grondelle, R. *Biochemistry* **1997**, *36*, 6855−6861.

(35) Zhou, H.; Boxer, S. G. *J. Phys. Chem. B* **1998**, *102*, 9139−9147.

(36) Zhou, H.; Boxer, S. G. *J. Phys. Chem. B* **1998**, *102*, 9148−9160.

(37) van Brederode, M. E.; van Mourik, F.; van Stokkum, I. H. M.; Jones, M. R.; van Grondelle, R. *Proc. Natl. Acad. Sci. U.S.A.* **1999**, *96*, 2054−2059.